



Identification of novel GPCR partners of the central melanocortin signaling

Yunpeng Li¹, Xiaozhu Wang^{2,***}, Liumei Lu¹, Meng Wang³, Yue Zhai¹, Xiaolu Tai¹, Diliqingna Dilimulati⁴, Xiaowei Lei¹, Jing Xu¹, Cong Zhang³, Yanbin Fu³, Shen Qu^{4,***}, Qingfeng Li^{3,****}, Chao Zhang^{3,*}

ABSTRACT

Objective: Homo- or heterodimerization of G protein–coupled receptors (GPCRs) generally alters the normal functioning of these receptors and mediates their responses to a variety of physiological stimuli *in vivo*. It is well known that melanocortin-3 receptor (MC3R) and melanocortin-4 receptor (MC4R) are key regulators of appetite and energy homeostasis in the central nervous system (CNS). However, the GPCR partners of MC3R and MC4R are not well understood. Our objective is to analyze single cell RNA-seq datasets of the hypothalamus to explore and identify novel GPCR partners of MC3R and MC4R and examine the pharmacological effect on the downstream signal transduction and membrane translocation of melanocortin receptors.

Methods: We conducted an integrative analysis of multiple single cell RNA-seq datasets to reveal the expression pattern and correlation of GPCR families in the mouse hypothalamus. The emerging GPCRs with important metabolic functions were selected for cloning and co-immunoprecipitation validation. The positive GPCR partners were then tested for the pharmacological activation, competitive binding assay and surface translocation ELISA experiments.

Results: Based on the expression pattern of GPCRs and their function enrichment results, we narrowed down the range of potential GPCR interaction with MC3R and MC4R for further confirmation. Co-immunoprecipitation assay verified 23 and 32 novel GPCR partners that interacted with MC3R and MC4R *in vitro*. The presence of these GPCR partners exhibited different effects in the physiological regulation and signal transduction of MC3R and MC4R.

Conclusions: This work represented the first large-scale screen for the functional GPCR complex of central melanocortin receptors and defined a composite metabolic regulatory GPCR network of the hypothalamic nucleuses.

© 2021 The Author(s). Published by Elsevier GmbH. This is an open access article under the CC BY-NC-ND license (<http://creativecommons.org/licenses/by-nc-nd/4.0/>).

Keywords MC3R; MC4R; GPCR; Single cell RNA-Seq; Energy homeostasis; Dimerization

1. INTRODUCTION

G protein–coupled receptors (GPCRs) are the largest family of cell membrane receptors, and nearly half of the molecular drugs in clinical medicine target GPCR signaling to treat various diseases of CNS, cardiovascular, metabolic systems, etc. [1,2]. Classical models hypothesize that GPCRs function as monomers. However, some recent studies acknowledge that GPCRs exist as homo- and heterodimers as well [3–5]. Heterodimerization could alter the ligand binding, second messenger activation and cell surface trafficking of multiple GPCR members [6–9]. The melanocortin system within the central nervous

system is known as a key neuronal pathway involved in appetite control and energy homeostasis [10–13]. Pro-opiomelanocortin (POMC) and agouti-related protein (AgRP) neurons serve the upstream endogenous ligands by projecting and modulating melanocortin-3 receptor (MC3R) and melanocortin-4 receptor (MC4R) signaling in multiple nucleuses of the hypothalamus [14,15]. GABA or glutamate could be released by POMC neurons as neurotransmitters [16]. In addition, the co-release of neuropeptide Y (NPY) and AgRP peptide to postsynaptic targets stimulated by ghrelin increases feeding, whereas leptin and insulin signaling decrease the appetite [17,18]. POMC and AgRP neurons exhibit similar activity profiles in

¹Department of Endocrinology and Metabolism, National Metabolic Management Center, Shanghai Tenth People's Hospital, Shanghai Key Laboratory of Signaling and Disease Research, Frontier Science Center for Stem Cell Research, School of Life Sciences and Technology, Tongji University, Shanghai, China ²Shanghai Key Laboratory of Signaling and Disease Research, Translational Medical Center for Stem Cell Therapy and Institute for Regenerative Medicine, Frontier Science Center for Stem Cell Research, School of Life Sciences and Technology, Shanghai East Hospital, Tongji University, Shanghai, China ³Department of Plastic and Reconstructive Surgery, Shanghai Institute of Precision Medicine, Shanghai Ninth People's Hospital, Shanghai Jiao Tong University School of Medicine, Shanghai, China ⁴Department of Endocrinology and Metabolism, National Metabolic Management Center, Shanghai Tenth People's Hospital, School of Medicine, Tongji University, Shanghai, China

****Corresponding author. E-mail: dr.liqingfeng@shsmu.edu.cn (Q. Li).

*Corresponding author. E-mail: zhangchao@shsmu.edu.cn (C. Zhang).

***Corresponding author. E-mail: qushenrc@hotmail.com (S. Qu).

**Corresponding author. E-mail: wangxiaozhu@tongji.edu.cn (X. Wang).

Received June 9, 2021 • Revision received August 3, 2021 • Accepted August 10, 2021 • Available online 14 August 2021

<https://doi.org/10.1016/j.molmet.2021.101317>

some aspects [19] and possess distinct physiological functions in the regulation of the central melanocortin system [20].

MC3R and MC4R are melanocortin receptors, members of a subfamily of the α group of class A $G\alpha_s$ protein-coupled receptors [21]. MC3R mRNAs are mainly expressed in the arcuate nucleus (ARH) and ventromedial hypothalamus (VMH), while MC4Rs are mainly expressed in the paraventricular hypothalamic nucleus (PVN), which is the crucial nucleus regulating energy homeostasis [22,23]. Both MC3R and MC4R are regulated by the antagonist/inverse agonist AgRP [24] and agonistic melanocortins, which include POMC-derived peptides ACTH and α -, β - and γ -melanocyte-stimulating hormone (MSH) [25–27]. MC3R-deficiency in mice altered the nutrient partitioning and led to an increase of the fat mass without a significant weight change [28]. In contrast, MC4R-deficient mice were reported to develop hyperphagia and early-onset severe obesity phenotype [29].

As a key component of metabolic regulation, non-ligand pharmacological modulation of MC3R and MC4R signaling has not been fully elucidated yet. Previous studies found that MC4R could form homodimer [30] and interacted with attractin-like protein (ALP) in mice [31]. In addition, MC4R signaling could be regulated in various species by interactions with MRAP and MRAP2, including alterations of ligand affinity and surface expression [32–37]. MC3R was able to interact with ghrelin receptor (GHSR) and the enhanced melanocortin-induced intracellular cAMP accumulation [38]. Based on these results, we hypothesized that some other unknown GPCRs could form functional heterodimers with MC3R or MC4R in the same neuron.

In addition to melanocortin receptors, a variety of other GPCRs were reported to regulate energy metabolism, and knockout of the corresponding GPCRs showed different degrees of obesity phenotype in mice [39]. For instance, HTR2C-deficient mice were hyperphagic and obese [40]. SSTR1 played a key role in the regulation of insulin secretion [41]. NPY1R and NPY5R served essential functions in controlling food intake [42].

Energy regulation is a complex and delicate physiological process involving the synergy of multiple genes and endocrine pathways [21,43,44]. However, understanding the remote interaction of genes from the distinct expression regions was not enough. In this study, MC3R and MC4R, the two key players that regulated energy metabolism, were examined to explore their novel endogenous GPCR partners, aiming to illustrate the complex regulatory network within the hypothalamic neurons. We first assessed the expression patterns of all mouse GPCRs in the integrative mouse hypothalamic single cell RNA-seq datasets and analyzed the function enrichment of selected GPCRs. The GPCRs with important functions in metabolism were further evaluated for expression correlation between various neuronal subtypes of the mouse hypothalamus. To further confirm the physical interaction of the selected GPCRs with MC3R and MC4R, we conducted co-immunoprecipitation screening and performed heterodimeric validation with multiple pharmacological assays *in vitro*. Finally, 23 and 32 novel GPCR were identified as novel physiological partners of MC3R and MC4R, respectively.

2. METHODS AND MATERIALS

2.1. Integrative analysis of GPCR network with melanocortin receptors of multiple hypothalamic single cell RNA-seq datasets

Four single cell RNA-seq (scRNA-Seq) datasets of the mouse hypothalamus were obtained from the NCBI Gene Expression Omnibus (GEO) at GSE87544 [45], GSE130597 [46], GSE74672 [47] and GSE125065 [48]. The analysis of these scRNA-Seq datasets was conducted using the R package Seurat [49]. In brief, the raw data

were filtered based on the detected gene number, counts and the percentage of mitochondrial/ribosomal genes. A total of 19,950 filtered cells were used in the subsequent analysis. To remove the batch effect of these datasets from different sources, we performed CCA integrative analysis using IntegratedData in Seurat. The PCA analysis, cell clustering and visualization steps were then conducted using Seurat with the default settings. The cell types of the identified cell clusters were annotated based on the known marker genes. For example, the neuron cells were identified based on some neuronal markers (Snap25, Syp, Tubb3 and Elavl2). We repeated the PCA analysis, cell clustering, visualization and cell type annotation steps only with the neuron cells, and six neuronal subtypes were identified in the mouse hypothalamus.

To visualize the expression pattern of GPCR members in our integrated mouse hypothalamus datasets, we generated a heatmap according to the expression level of each GPCR in each of the identified cell types (only the detected GPCRs were included). The GPCRs detected in the integrated hypothalamus scRNA-Seq datasets underwent Gene Ontology (GO) and Biological Process (BP) enrichment analysis with the R package clusterProfiler [50]. Functional annotations with a p-value <0.05 (FDR corrected) were considered statistically significant. To evaluate the expression correlation of the functionally important GPCRs and melanocortin receptors, we further performed the pairwise Pearson Correlation Coefficient Analysis in all six neuronal subtypes using the R package corr [51].

2.2. Reagents, plasmids and antibodies

Mouse MC3R, MC4R and GPCRs were cloned from the mouse brain cDNA library, and all the fragments were constructed into vector pcDNA3.1 (+) with an HA or FLAG protein tag. Agonist α -melanocyte stimulating hormone (α -MSH) and antagonist SHU9119 were purchased from Genescript (Nanjing, China). Mouse monoclonal anti-HA (Sigma—Aldrich, MO, USA), anti-Flag (ABclonal Biotech, China) and horseradish peroxidase (HRP)-conjugated antibodies against mouse and rabbit (ABclonal Biotech, China) were used for the subsequent experiments.

2.3. Cell culture and transfection

HEK293 cells were maintained in Dulbecco's Modified Eagle Medium (DMEM) with 10% (v/v) fetal bovine serum (FBS) and 1% (v/v) penicillin-streptomycin. CHO cells were maintained in Dulbecco's Modified Eagle Medium/F-12 medium supplemented with 5% (v/v) FBS and 1% (v/v) penicillin-streptomycin. Cells were then incubated at 37 °C in humidified air containing 5% CO₂. Transfection was carried out with Viafect Transfection Reagent (Promega, WI, USA) following the manufacturer's protocols. The total plasmid concentrations were kept identical across all transfections by adding empty pcDNA3.1 (+) vector.

2.4. Western blotting and immunoprecipitation

HEK293 cells (1×10^6) were plated in 60 mm dishes and transfected with 2 ug of the indicated plasmid the following day. After 48 h of transfection, followed by washing with PBS, cells were then lysed with lysis buffer (0.75% Triton-X, 50 mM Tris-HCl pH 7.9, 150 mM NaCl and proteinase inhibitor cocktail, Roche) for 1 h at 4 °C. The insoluble fragments were removed from the cell lysate by centrifugation. Denatured proteins were separated by 12% SDS-PAGE gels and transferred to nitrocellulose membranes. Immunoblotting was conducted with mouse anti-HA or rabbit anti-Flag antibody as the primary antibody and then with goat anti-mouse or goat anti-rabbit antibody linked with horseradish peroxidase (HRP) as the second

antibody. Proteins were visualized with enhanced chemiluminescence reagents following the manufacturer's protocol. ImageQuant LAS 4000 system (General Electric Company, CT, USA) was used to capture images.

MC3R and MC4R (1.0 µg of DNA/60 mm dishes) with or without GPCRs (1.0 µg of DNA/60 mm dishes) were co-transfected into HEK293 cells. After 48 h of transfection, cells were lysed and centrifuged, and supernatants were then incubated overnight at 4 °C with the mouse anti-HA or rabbit anti-Flag antibody at 1/5000 dilution. Protein A/G agarose beads bound to immune complexes were washed three times and resuspended in loading buffer with 5% β-mercaptoethanol. The protein complexes were denatured in 85 °C for 10 min in metal bath. Samples were analyzed on western blots as described above.

2.5. Intracellular CRE-luc cAMP measurement

The accumulation of intracellular cAMP was measured using HEK293 cells cultured in 24-well plates and transfected with indicated plasmids at a cell density of 50–60%. CRE-luc assays were performed using the Dual-Luciferase Reporter Assay System (Promega). A total of 300 ng DNA was added to each group, with 60 ng pCRE-luc and 30 ng pRL-TK constant and empty pcDNA3.1 (+) vector. After 24 h of transfection, cells continued incubation for 4 h at 37 °C in medium with α-MSH in serum-free DMEM supplemented with 0.1% bovine serum albumin (concentration from 10⁻¹¹ M to 10⁻⁶ M). For competitive binding assay, cells were treated with a fixed concentration of α-MSH (10⁻⁸ M) and different concentrations of SHU9119 in serum-free DMEM. Firefly and Renilla luciferase activities were measured using

a Spectramax M5 multimode plate reader. Firefly luciferase activities were normalized to Renilla luciferase activities.

2.6. Cell surface ELISA

Twelve-well plates were pretreated with polylysine solution before culturing HEK293 cells were transfected with indicated plasmids the next day. After 36 h of transfection, cells were first washed with D-PBS three times for 5 min each time, then fixed for 15 min with 4% paraformaldehyde at room temperature and blocked for 30 min with 5% milk in PBS (Surface-expression measurement) or 5% milk in RIPA buffer (150 mM NaCl, 50 mM Tris, 1 mM EDTA, 1% Triton X-100, 0.1% SDS, 0.5% sodium deoxycholate, pH 8.0) (total-expression measurement) at room temperature. After being incubated for 90 min, 1:4000 mouse anti-HA or anti-FLAG monoclonal antibodies were washed three times with PBS and incubated with 1:6000 HRP-conjugated anti-mouse antibodies for 1 h. The reaction was terminated with 5% sulfuric acid after being washed three times with PBS and incubated with TMB for 40 min. The absorbance was recorded at 450 nm on Spectramax M5 multimode plate reader.

2.7. Immunofluorescence assay

YFP-F1 and YFP-F2 of whole YFP fragments were utilized to construct plasmids at the C-terminus of GPCRs. CHO cells were cultivated in a 12-well plate with slides pretreated with poly-D-lysine. After 24 h of transfection, slides were washed twice with D-PBS and fixed with 4% paraformaldehyde for 15 min, incubated in PBS solution containing 0.1% Triton and 5% goat serum for 1 h, washed three times with PBS

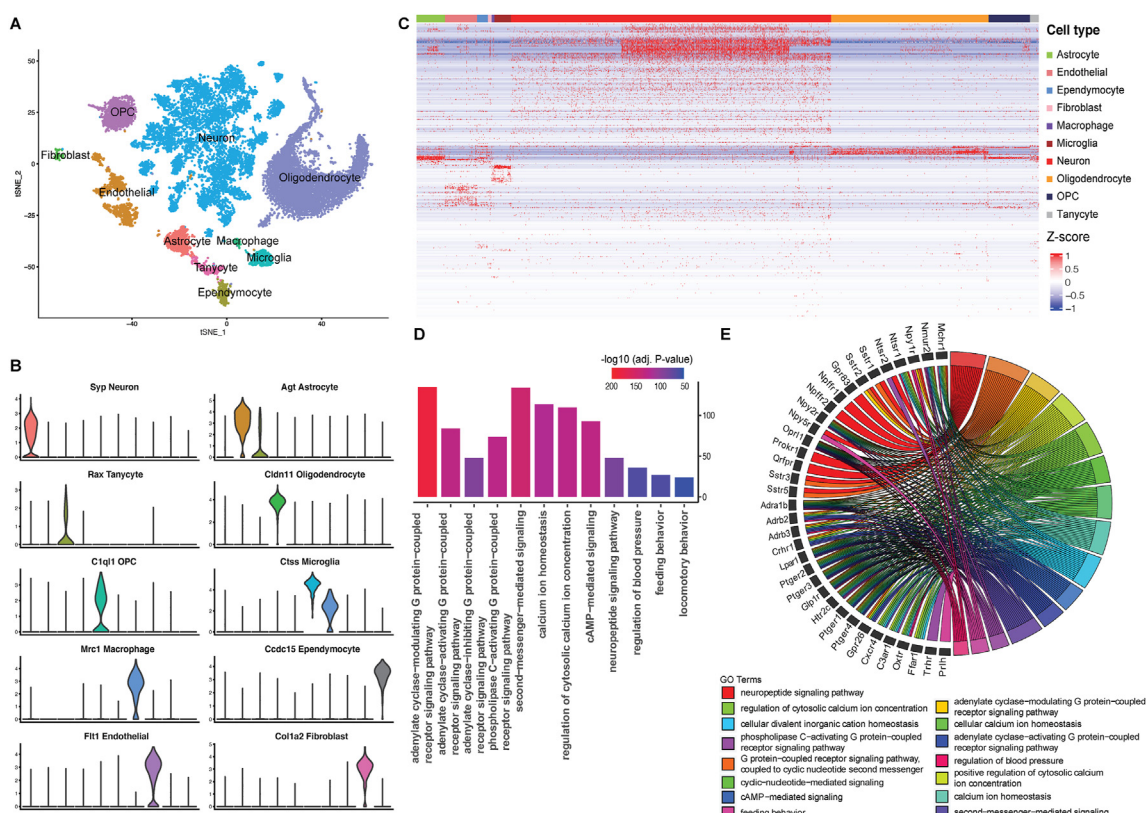


Figure 1: Co-expression and functional enrichment analysis of GPCR families in the mouse hypothalamus. (A) tSNE plot identification of 10 cell types in the integrative single cell RNA-seq datasets of the mouse hypothalamus; (B) Expression level of the well-known genetic markers for each cell type in the mouse hypothalamus; (C) Expression profiles of the emerging mouse GPCRs, which reveal an enriched pattern in the mouse hypothalamic neurons; (D) GO biological process (BP) functional enrichment analysis of the GPCRs detected in the mouse hypothalamus; (E) Signal pathway enrichment of the functionally important GPCRs.

and incubated in PBS solution containing anti-FLAG antibody at 1:2000, 0.1% Tween and 5% goat serum overnight. Slides were then washed 3 times and incubated in PBS solution containing 0.1% Tween, 5% goat serum and 1:1000 secondary antibody Alexa Fluor594 (Abcam) for 2 h at 37 °C. DAPI was added to the glass slice and analyzed by a Nikon laser confocal microscope.

3. RESULTS

3.1. Expression pattern of the GPCR network in the mouse hypothalamus at single cell resolution

As one of the most complex brain regions, the hypothalamus is well studied for its regulation of energy homeostasis. With the advance of scRNA-Seq technology, we now can identify the expression pattern of any genetic network within the hypothalamus at single cell resolution. In this study, we integrated four publicly available scRNA-Seq datasets of the mouse hypothalamus to reveal the expression patterns of Mc3r/Mc4r and all mouse GPCRs. We identified a total of 10 cell types in the integrated mouse hypothalamic transcriptome data, including 9,427 neurons, 738 astrocytes, 348 tanycytes, 5,931 oligodendrocytes, 1,221 oligodendrocyte precursor cells (OPCs), 437 microglia, 95 macrophages, 362 ependymocytes, 1,254 endothelial cells, and 137 fibroblasts (Figure 1A). Cell type annotations were based on the well-known genetic markers, and their expression levels in each cell type were illustrated in Figure 1B. To screen the expression levels of all GPCRs in different cell types of the mouse hypothalamus, we generated an expression heatmap of all expressed mouse GPCRs, indicating that a total of 294 GPCRs (including Mc3r and Mc4r) were detected in different hypothalamic cells, and most of them enriched in neurons (Figure 1C).

To identify the function of these detected GPCRs in the mouse hypothalamus, we further performed functional enrichment analysis according to the GO biological process database using the R package clusterProfiler [50] (Figure 1D, E), and revealed many important signal pathways involved in metabolic regulation of MC3R and MC4R, such as adenylate cyclase-modulating G protein-coupled receptor signaling and G protein-coupled peptide receptor activity. Therefore, we selected 43 GPCRs enriched in those metabolism-related pathways to further validate their heterodimerization with MC3R/MC4R *in vitro* (Tables 1 and 2).

As most emerging GPCRs were enriched in neurons of the mouse hypothalamus, we further identified 6 neuronal subtypes (GABA neuron, Glu neuron, Npy neuron, Hcrt neuron, Pmch neuron and Avp neuron) based on the significant markers identified using the Wilcox method in Seurat (Figure 2A, B). We found that Pomp, Agrp, Mc3r and Mc4r were expressed in all of these neuronal subtypes (Figure 2C). To evaluate the expression correlation of these 43 selected GPCRs and Mc3r/Mc4r, we conducted pairwise Pearson Correlation Coefficient Analysis in each neuronal subtype. The expression correlation network of these GPCRs indicated that they were more correlated with Mc3r and Mc4r in Npy, Hcrt, Pmch and Avp neurons than that in GABA and Glu neurons (Figure 2D).

3.2. Assessment of heterodimerization of GPCRs with MC3R or MC4R

GPCR heterodimerization has been proved to regulate the molecular function of GPCR protomers. Based on the results of mouse hypothalamus single cell RNA-seq integrative and functional enrichment analysis, 43 GPCRs were selected for the subsequent immunoprecipitation assay to verify heterodimerization with MC3R and MC4R *in vitro*. Our

Table 1 — Summary of pharmacological regulation of MC3R signaling by selective GPCRs.

NO	Gene Name	Maximal response	Antagonism	Surface translocation	NO	Gene Name	Maximal response	Antagonism	Surface translocation	NO	Gene Name	Maximal response	Antagonism	Surface translocation
1	ADRA1B	NT	NT	↑	16	NTSR1	↑	NS	↑	31	HTR2C	—	—	—
2	ADRB2	NT	NT	NS	17	NTSR2	↑	NS	↑	32	NPFPR1	—	—	—
3	ADRB3	NT	NT	↓	18	OXTR	↓	↑	↑	33	NPFPR2	—	—	—
4	CRHR1	NT	NT	NS	19	PRLH	↑	↑	↑	34	NPY2R	—	—	—
5	CXCR4	↑	NS	↑	20	PTGER2	NT	NT	↑	35	NPY5R	—	—	—
6	C3AR1	↓	↑	↑	21	PTGER3	↑	↑	NS	36	OPRLR	—	—	—
7	GPRC5B	NT	NT	↑	22	SSTR1	↓	↑	NS	37	PROKR1	—	—	—
8	GPR19	↑	NS	↓	23	SSTR2	NS	NS	↑	38	PTGER1	—	—	—
9	GPR88	↑	—	↓	24	FFAR1	—	—	—	39	PTGER4	—	—	—
10	GPR146	NT	NT	↑	25	GHR	—	—	—	40	QRFP	—	—	—
11	GPR150	NT	NT	↓	26	GLP1R	—	—	—	41	SSTR3	—	—	—
12	LPAR1	↑	↑	↑	27	GPR26	—	—	—	42	SSTR5	—	—	—
13	MCHR1	↑	↓	↑	28	GPR63	—	—	—	43	TRHR	—	—	—
14	NMUR2	↓	↑	↑	29	GPR75	—	—	—	44				
15	NPY1R	↓	↑	↓	30	GPR83	—	—	—	45				

NT: not tested in this experiment; NS: no significant difference; ↑: up-regulation; ↓: down-regulation; —: negative results.

Table 2 — Summary of pharmacological regulation of MC4R signaling by selective GPCRs.

NO	Gene Name	Maximal response	Antagonism	Surface translocation	NO	Gene Name	Maximal response	Antagonism	Surface translocation	NO	Gene Name	Maximal response	Antagonism	Surface translocation
1	ADRB2	NT	NT	↑↓	16	NPFFR1	↑↓	↑	↑	31	SSTR3	↑↓	↑	↓
2	ADRB3	NT	NT	↓	17	NPY1R	↓	NS	↓	32	TRHR	↓	NS	NS
3	CRHR1	NT	NT	NS	18	NPY2R	NS	NS	↓	33	ADRA1B	—	—	—
4	CXCR4	↑↓	↑	↓	19	NPY5R	↓	↑	↑	34	FFAR1	—	—	—
5	C3AR1	NT	NT	↓	20	NTSR1	↓	NS	↓	35	GHR	—	—	—
6	GPRC5B	↓	NS	↓	21	NTSR2	NS	NS	NS	36	GLP1R	—	—	—
7	GPR26	NT	NT	↓	22	OXTR	↓	NS	↓	37	GPR19	—	—	—
8	GPR63	↓	NS	↓	23	PROKR1	↓	NS	↓	38	GPR75	—	—	—
9	GPR88	—	NS	↓	24	PTGER1	NS	↑	↑	39	GPR83	—	—	—
10	GPR146	↑	NS	↓	25	PTGER2	NT	NT	↓	40	NPFFR2	—	—	—
11	GPR150	NT	NT	NS	26	PTGER3	↓	↑	↓	41	OPRLR	—	—	—
12	HTR2C	↑	↓	↑	27	PTGER4	NT	NT	↓	42	PRLH	—	—	—
13	LPAR1	NT	NT	NS	28	QRFP	NT	NT	↓	43	SSTR5	—	—	—
14	MCHR1	↓	NS	NS	29	SSTR1	↓	↑	↑	44	—	—	—	—
15	NMUR2	↓	↑	NS	30	SSTR2	↓	↑	↓	45	—	—	—	—

NT: not tested in this experiment; NS: no significant difference; ↑: up-regulation; ↓: down-regulation; —: negative results.

results identified that 23 and 32 GPCRs positively interacted with MC3R and MC4R, respectively. Notably, different members of the single GPCR family exhibited distinct interactive profiles with MC3R and MC4R. For instance, our bioinformatic analysis found that the Neuropeptide Y receptors (NPYRs) were expressed in the mouse hypothalamus and responsible for regulating feeding behavior. However, the immunoprecipitation assay indicated that MC3R only interacted with NPY1R (Figure 3E), whereas MC4R interacted with NPY1R, NPY2R and NPY5R (Figure 3P–R). Both MC3R and MC4R could interact with the Somatostatin receptor (SSTR) (Figure 3A–B, M–O) and Prostaglandin E2 receptor (PTGER) families (Figure 3C–D, S–U). Other co-immunoprecipitation results are shown in Supplementary Figure 1.

To further confirm the functional heterodimer complex of identified GPCRs with MC3R or MC4R on the cell surface, we performed a complementary YFP luminescent assay in the live cells. A schematic representation of configurations in which MC4R and GPCR fused with YFP fragments on the plasma membrane is shown in Figure 4A. We applied fluorescence complementation assay for MC3R, MC4R and 23 identified positive GPCRs, and a clear YFP fluorescence distribution was observed on the cell membrane (Figure 4B–L, Supplementary Figure 2). These results further confirmed that the identified GPCR partners from immunoprecipitation assay could form functional heterodimers with MC3R and MC4R on the cell membrane *in vitro*.

3.3. Pharmacological effect of GPCR partners on $\text{G}\alpha_s$ signaling of MC3R and MC4R

To examine the effect of identified GPCR partners on MC3R and MC4R signaling pathways, we performed CRE-luciferase reporter

assay to detect the intracellular cAMP accumulation stimulated by its natural agonist. In the co-transfection system, we transfected a fixed amount of MC3R or MC4R with different amount of GPCRs. Based on previous studies of GPCR signaling, we chose $\text{G}\alpha_s$ -coupled receptors to verify the pharmacological effect of MC3R and MC4R on the cAMP accumulation. The results of CRE-luciferase reporter assay suggested that these GPCRs exhibited distinct effects on MC3R signaling. For instance, C3AR1, OXTR, GPR88, NMUR2 and SSTR1 exhibited dose-dependent inhibitory effects on MC3R signaling (Figure 5A, B, D, G, H). In particular, the cAMP accumulation of MC3R activation was nearly blocked in the presence of OXTR (Figure 5B). In contrast, NTSR1, NTSR2 and MCHR1 significantly increased the maximal stimulated efficacy of MC3R (Figure 5I, C, E). Beyond that, GPR19, CXCR4, PRLH and PTGER3 slightly enhanced cAMP accumulation, and SSTR2 had no significant effect (Supplementary Figure 3A, B, C, D, F).

Unlike MC3R, only GPR146 and HTR2C could increase the cAMP accumulation of MC4R stimulated by α -MSH (Figure 5M, O), and HTR2C altered constitutive activity of MC4R. Other GPCRs could reduce the α -MSH response of MC4R, such as GPR63, NPFFR1 and SSTR1 (Figure 5K, R, Supplementary Figure 3J). Similar to the effect of OXTR on MC3R signaling, it also significantly blocked the $\text{G}\alpha_s$ pathway of MC4R signaling (Figure 5T). Intriguingly, CXCR4 and PTGER3 showed opposite effects on MC4R versus MC3R signaling (Figure 5J and Supplementary Figure 3L). The underlying mechanisms of the opposite regulatory effects of these GPCRs on MC3R and MC4R need further exploration. Taken together, our results demonstrate that some GPCRs present significant pharmacological effects on the signaling pathways

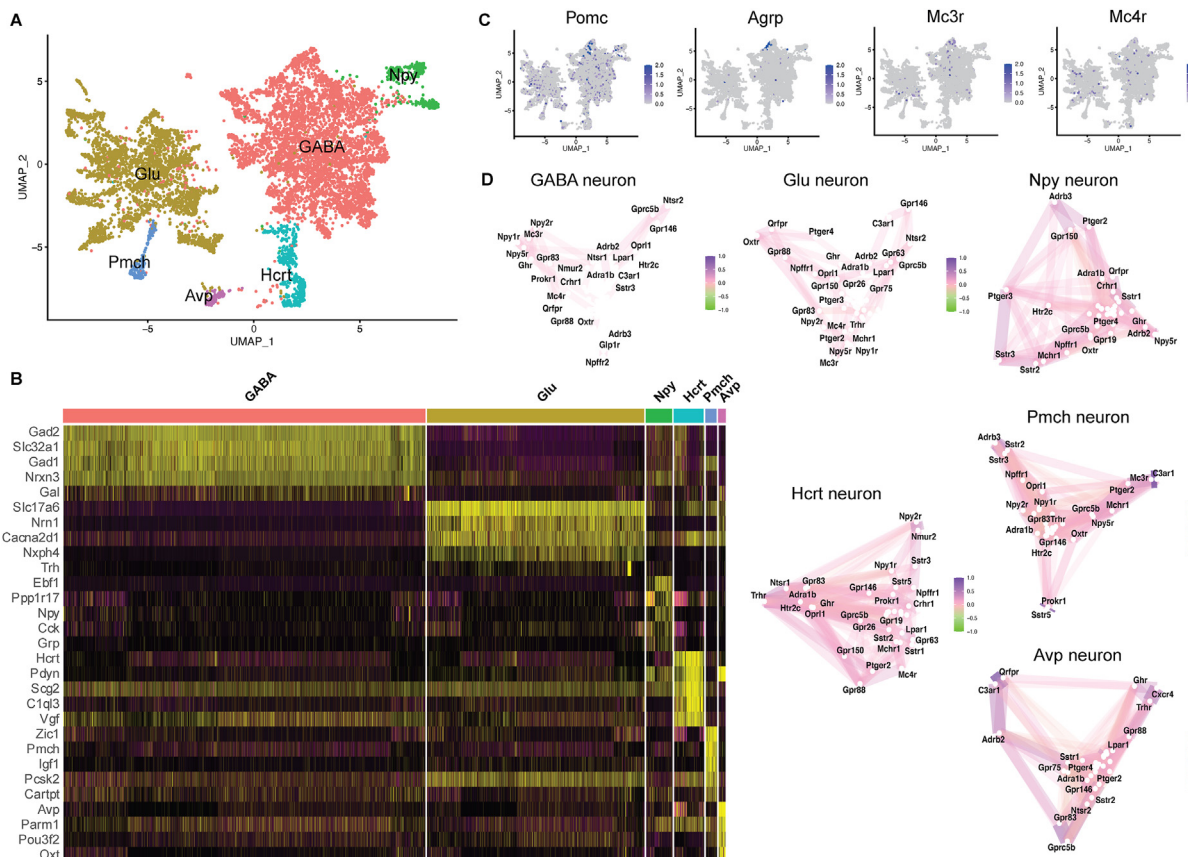


Figure 2: Correlation analysis of the functionally important GPCRs in neuronal subtypes of the mouse hypothalamus. (A) UMAP plot identification of 6 neuronal subtypes of the mouse hypothalamus; (B) Expression level of the well-known genetic markers for each of the neuronal subtypes; (C) Expression levels of Pomc, Agrp, Mc3r and Mc4r among different neuronal subtypes; (D) Correlation network of the functional important GPCRs in 6 neuronal subtypes.

of MC3R and MC4R, suggesting that these GPCRs might cause the alteration of the binding affinity of natural ligands or G proteins to MC3R and MC4R.

3.4. Alteration of antagonism of MC3R or MC4R in presence of GPCR partners

To examine the alteration of antagonism of MC3R or MC4R in the presence of the identified GPCR partners, we performed competitive binding assay of antagonist SHU9119 (10^{-6} – 10^{-11} M) in the presence of a fixed concentration of α -MSH (10^{-8} M). We found that some GPCRs could increase the inhibition of MC3R signaling by SHU9119, such as SSTR1, GPR88 and LPAR1 (Figure 6B, D, E), while other GPCRs (NTSR1, NTSR2 and CXCR4) did not change the response to SHU9119 (Supplementary Figure 4A, B, E). Intriguingly, only MCHR1 slightly reduced the response of MC3R (Figure 6F). As with the results of MC3R, some GPCRs increased MC4R signaling to SHU9119, including CXCR4, NMUR2 and NPFFR1 (Figure 6J, N, O). However, HTR2C reduced the MC4R response to SHU9119 (Figure 6L). The IC50 statistical analysis of other GPCRs was shown in Table 3 and Table 4. These results suggest that these GPCRs in heterodimer could affect the antagonism of MC3R and MC4R *in vitro*.

3.5. Influence of the surface translocation of MC3R and MC4R by GPCR partners

Previous studies demonstrated that the heterodimers of GPCRs may affect receptor trafficking and expression level on the cell surface. Based on the cAMP accumulation results of MC3R and MC4R, we

hypothesized that the formation of heterodimers might alter MC3R and MC4R trafficking. We first constructed MC3R, MC4R and GPCRs with different protein tags at the N-terminal, co-transfected them with GPCRs at different ratios, then quantified the cell surface expression level by non-permeabilized ELISA assay. Strong inhibitory effects of C3AR1, GPR88, GPR150, GPR19 and NPY1R were identified on the cell surface expression of MC3R (Figure 7A,B and Supplementary Figure 5D, H, J). NMUR2, CXCR4, OXTR, SSTR2 and GPRC5B revealed a dose-dependent stimulatory effect on MC3R membrane translocation, while MC3R presented the opposite effect on these GPCRs (Figure 7D,H, I and Supplementary Figure 5C and F). The effects of NTSR1, NTSR2, CXCR4 and PRLH (Figure 7E,F, H and Supplementary Figure 5B) on the surface expression of MC3R membranes may be the key reason for changing the maximum potency of MC3R activation. Similarly, we also found inhibitory effects of many GPCRs, including PTGER4, NPY2R and GPRC5B, on MC4R membrane translocation (Figure 7M, P and Supplementary Figure 6R). The obvious inhibition of OXTR, NPY1R, CXCR4, GPR63 and GPR88 on cAMP accumulation of MC4R may result from the reduction of membrane expression of MC4R proteins (Figure 7J, L, R and Supplementary Figure 6D and J).

4. DISCUSSION

The central melanocortin system plays an important role in appetite control and energy homeostasis. Lack of MC3R was reported to increase fat mass and improve feed efficiency, suggesting an impact on

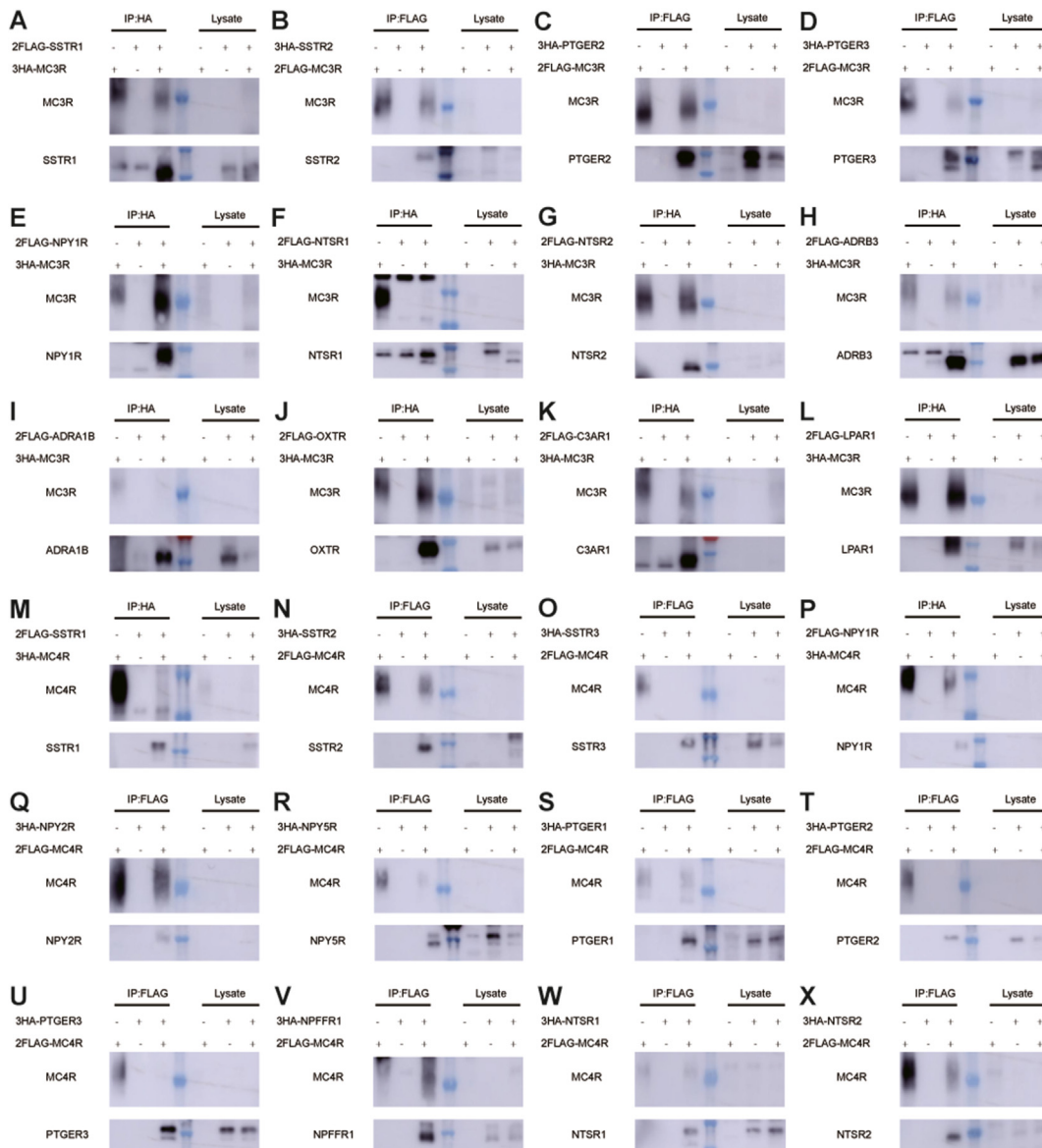


Figure 3: Co-immunoprecipitation analysis of selective GPCRs with MC3R or MC4R. MC3R, MC4R and GPCRs are labeled with HA and FLAG tags, respectively. (A–L) Selective GPCRs are pulled down by MC3R and co-immunoprecipitation analysis of MC3R and GPCRs are performed; (M–X) Selective GPCRs are pulled down by MC4R and co-immunoprecipitation analysis of MC4R and GPCRs are performed. Co-IP results of other GPCRs are shown in [Supplementary Figure 1](#).

nutrient partitioning and feeding behavior [52–54]. MC4R deficiency increased food intake and decreased energy expenditure, which ultimately led to severe early-onset obesity syndrome [55,56]. Although MC3R and MC4R served the key determinants for physiological metabolic homeostasis, the broad regulatory network that interacted with other GPCRs was poorly understood. In some reported cases, heterodimerization was required for efficient agonist binding and downstream signaling of GPCR activation. Therefore, screening for new GPCR partners interacting with MC3R or MC4R has become more important.

Large-scale blind screening of proteins that interact with MC3R and MC4R was time consuming and economically costly. In this study, we employed four published mouse hypothalamus single cell RNA-seq datasets to narrow down the range of candidate GPCRs by performing integrative bioinformatic analysis. The expression heatmap

revealed an enriched expression pattern of many GPCRs (including Mc3r and Mc4r) in mouse hypothalamic neurons, suggesting that they may interact with each other within the same cell. The functional enrichment analysis of these detected GPCRs (including Mc3r and Mc4r) indicated their involvement in many important metabolic pathways, such as adenylate cyclase-modulating GPCR signaling pathway, second messenger mediated signaling, cAMP-mediated signaling, and feeding behavior. The functionally important GPCRs involved in metabolic signaling pathways were selected for further evaluation.

We further analyzed and identified 6 neuronal subtypes in the integrative mouse hypothalamic single cell transcriptome. Pomp, Agrp, Mc3r and Mc4r were widely expressed with no subtype-specific enrichment pattern in mouse hypothalamic neurons. Previous studies had already elucidated the opposite effects of AgRP and POMC

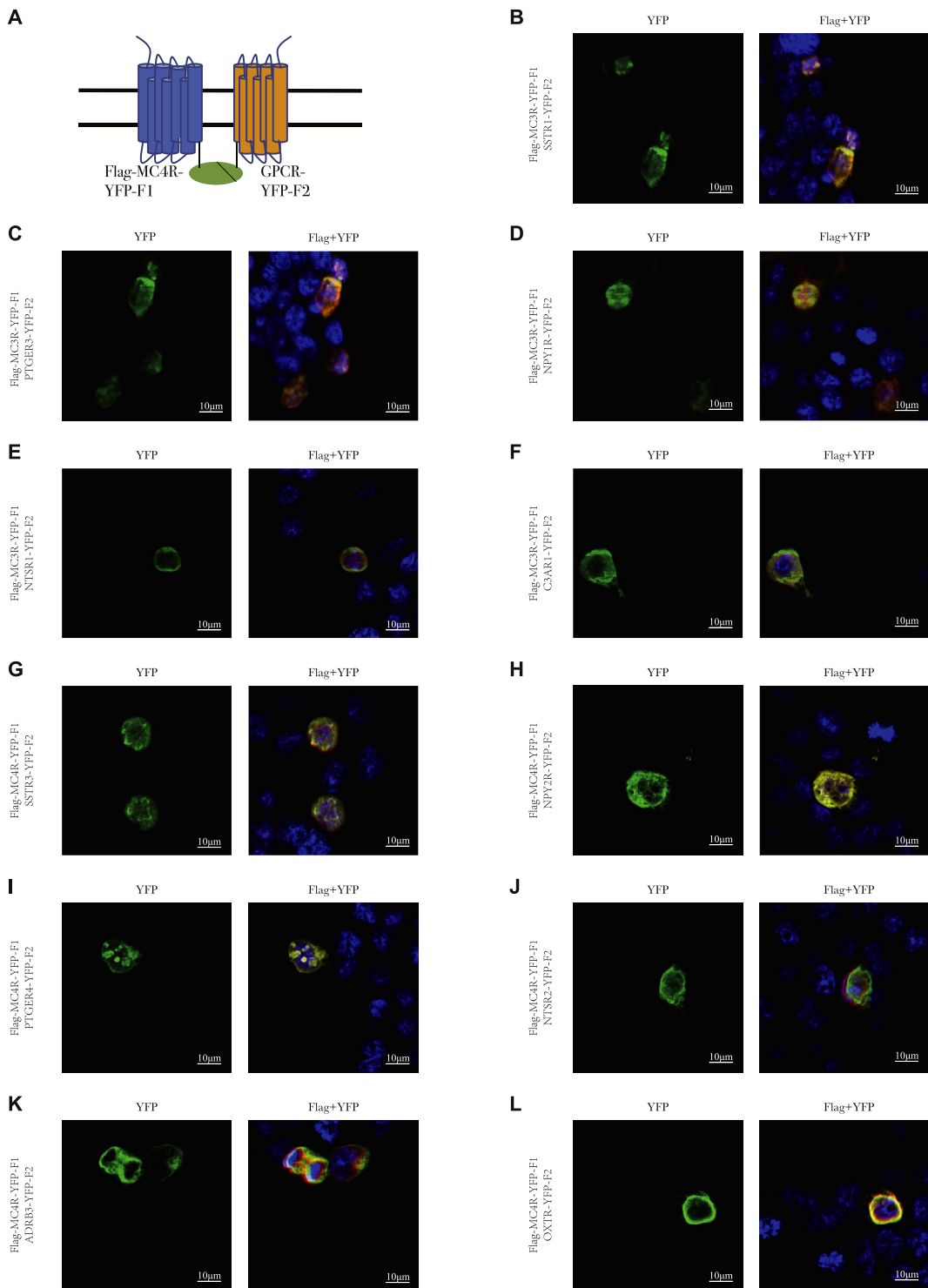


Figure 4: Complementary YFP luminescent assay of selective GPCRs with MC3R or MC4R. (A) Schematic diagram of MC4R and GPCRs on the plasma membrane. N-terminal of MC3R or MC4R is labeled with FLAG tag and C-terminal is fused to YFP-F1; C-terminal of GPCRs is fused to YFP-F2. YFP fluorescence (green) and Flag fluorescence (red) represent the formation of heterodimer on the cell surface; (B–F) The complementary YFP luminescent illustration of MC3R with selective GPCRs; (G–L) The complementary YFP luminescent illustration of MC4R with selective GPCRs.

neurons toward feeding and metabolism regulation [57]. POMC neurons could receive inhibitory inputs from GABAergic AgRP neurons [58], while AgRP neurons could send their axonal projections to PVH [59]. These studies demonstrated the important role of POMC and

AgRP neurons in appetite control and energy homeostasis. The expression correlation analysis of those functionally important GPCRs with Mc3r/Mc4r suggested that they may interact with each other in the same cell, especially in the Npy, Hcrt, Pmch and Avp neurons.

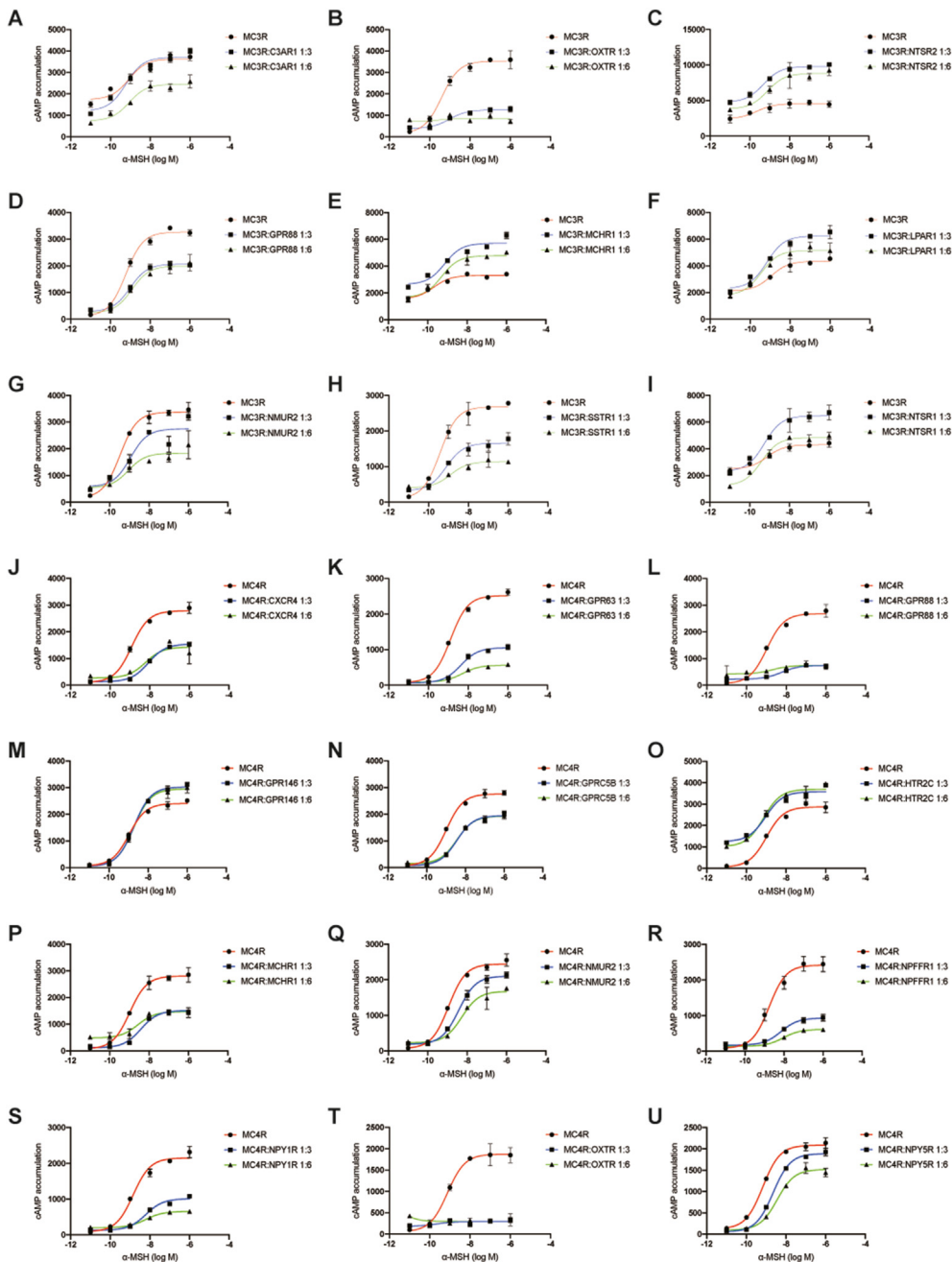


Figure 5: Pharmacological effect of the presence of selective GPCRs on the G_{α_s} cAMP signaling of MC3R or MC4R. (A–I) cAMP accumulation of MC3R stimulated by α -MSH in presence of two dosages of selective GPCRs; (J–U) cAMP accumulation of MC4R stimulated by α -MSH in presence of two dosages of selective GPCRs.

Based on the bioinformatic analysis, we finally selected 43 mouse GPCRs as putative candidates that may interact with MC3R and MC4R. To verify the actual interaction, co-immunoprecipitation assay, CRE-luciferase reporter assay, competitive binding assay and cell surface translocation experiments were performed. Co-immunoprecipitation had been widely used as an important method of GPCR heterodimerization, and our results showed that 23 and 32 GPCRs positively interacted with MC3R and MC4R, respectively. However, false-positive results of GPCR heterodimers *in vitro* may still be inevitable, although we reduced the transfection quantity and washed Protein A+G agarose thoroughly to minimize false-positive results. In addition, we used

complementary YFP luminescent assay to validate the co-immunoprecipitation results, which further confirmed the identified GPCR heterodimerization with MC3R and MC4R in live cells. These GPCRs forming heterodimers with MC3R or MC4R were previously reported to participate in the energy metabolism and hemostasis. For instance, SSTR1 knockout mouse exhibited reduced body weight and decreased levels of insulin secretion [41], which was contrary to the phenotype of MC3R or MC4R knockout mice. The PTGER family was barely found in the brain region, but highly expressed in the kidneys, lungs and ileum, implying physiological regulation in other organs [60,61]. OXTR and MCHR1 were mostly expressed in the brain,

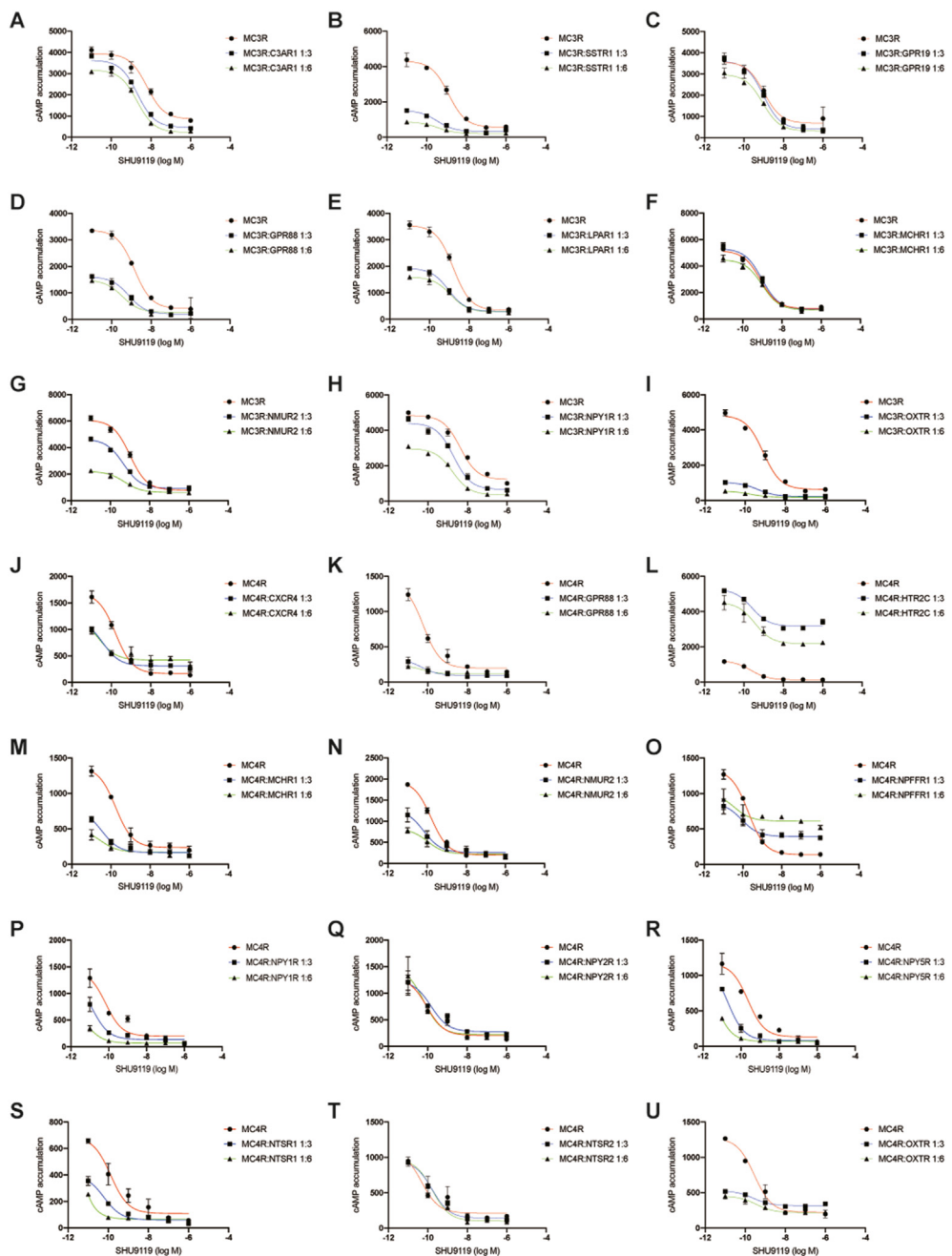


Figure 6: Competitive binding assay of selective GPCRs with MC3R and MC4R. (A–I) Competitive binding of the antagonist SHU9119 with EC80 α -MSH of MC3R in the presence of two dosages of selective GPCRs; (J–U) Competitive binding of the antagonist SHU9119 with EC80 α -MSH of MC4R in the presence of two dosages of selective GPCRs.

and knockout models generated different types of obese phenotypes [62,63]. Here we discovered that HTR2C could form heterodimers with MC4R, but not MC3R, *in vitro* (Supplementary Figure 1). This finding was supported by several studies in which HTR2C and MC4R exhibited similar roles in regulating energy homeostasis [64]. Moreover, both HTR2C and MC4R were highly expressed in the hypothalamic nucleus, and the HTR2C expressed in the POMC neurons mediated the effect of serotonergic compounds on food intake. In addition, MC3R and MC4R could also bind to orphan receptors, among which GPR88 regulated energy homeostasis and body composition [65], GPR146 regulated blood cholesterol levels and GPRC5B acted as a negative

regulator of insulin secretion [66,67]. Taken together, our findings provide new implications for the physiological relevance of these identified GPCRs and MC3R/MC4R in the central regulation of energy balance.

Furthermore, we found that the heterodimers of GPCRs with melanocortin receptors influenced the $G\alpha_s$ signaling, antagonism and membrane expression of MC3R and MC4R to different degrees, indicating that in some cases the actual physical interaction with GPCRs could lead to functional activation or inactivation of melanocortin cascades *in vitro*. Numerous studies have reported that heterodimers of GPCR members resulted in the alteration of downstream signaling, competitive binding of

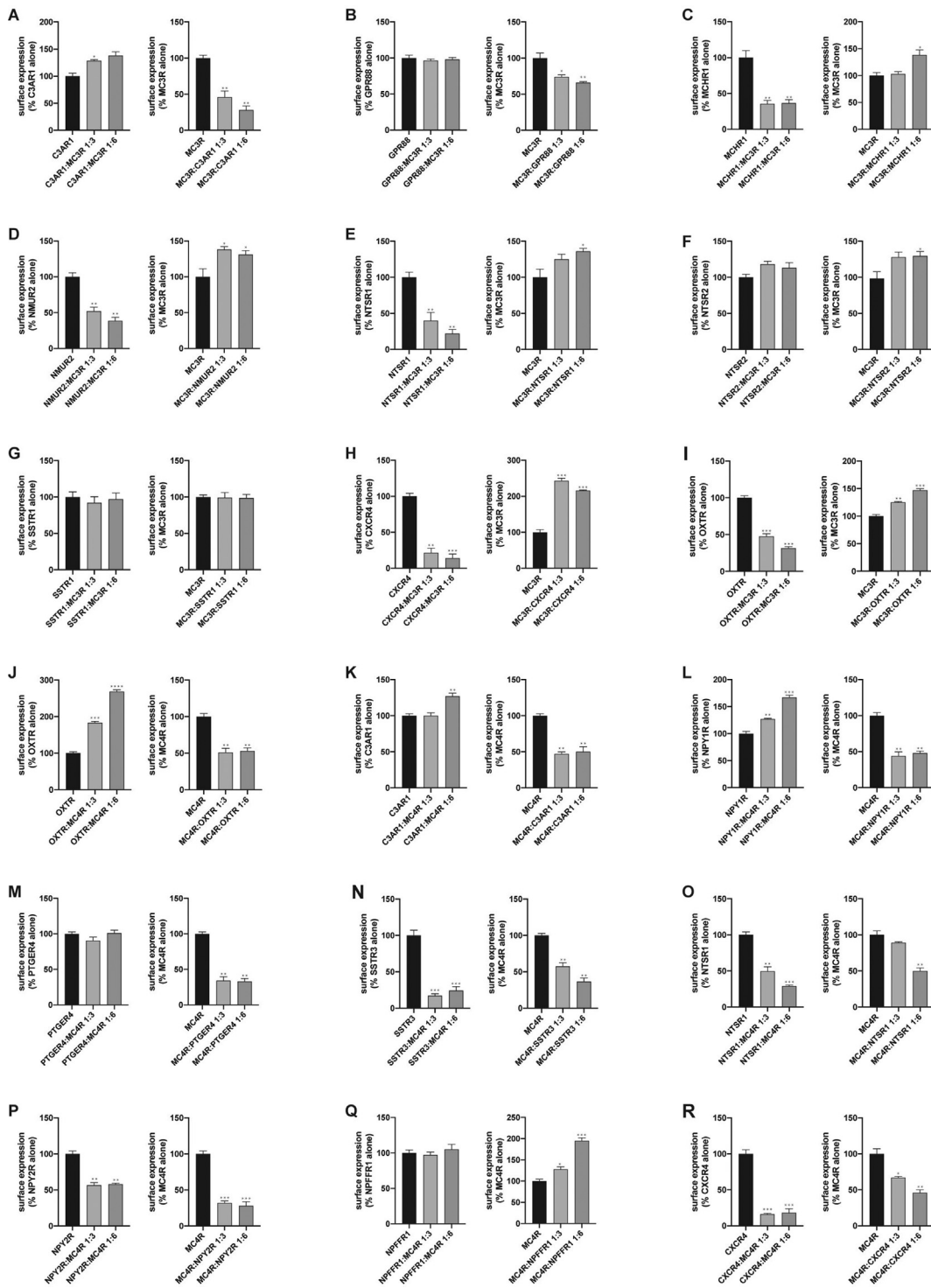


Figure 7: The surface expression measurement of MC3R or MC4R in presence of the selective GPCRs. (A–I) Non-permeabilized ELISA is performed to measure the surface expression of MC3R in the presence of two dosages of selective GPCRs that form heterodimers with MC3R; (J–R) Non-permeabilized ELISA is performed to measure the surface expression of MC4R in the presence of two dosages of selective GPCRs that form heterodimers with MC4R. *P < 0.05; **P < 0.01; ***P < 0.001.

multiple ligands and membrane translocation efficacy. For instance, the heterodimer of MC3R and GHSR generated a mutual opposite effect on their signal modulation, whereas GHSR increased cAMP accumulation of MC3R stimulated by α -MSH [38]. In our study, we found that MCHR1, LPAR1 and NTSR1 could significantly improve the MC3R signaling

transduction, but the underlying molecular mechanisms remained unknown. The cause might involve changes in the helical structure of the protein caused by special binding sites [68] or alterations in G protein–coupling mediated by agonists [69]. Additionally, NTSR2 could not only increase the maximum activation potency of MC3R, but also increase the

Table 3 – Statistical analysis of competitive binding curve of MC3R.

	LogIC50			P value	
	1:0	1:3	1:6	1:0 vs 1:3	1:0 vs 1:6
MC3R:C3AR1	−8.19 ± 0.06	−8.69 ± 0.06	−8.69 ± 0.07	< 0.05	< 0.05
MC3R:GPR88	−8.84 ± 0.01	−9.14 ± 0.13	−9.48 ± 0.16	NS	< 0.05
MC3R:LPAR1	−8.79 ± 0.01	−9.04 ± 0.02	−8.94 ± 0.02	< 0.01	< 0.01
MC3R:MCHR1	−9.10 ± 0.02	−9.03 ± 0.01	−9.01 ± 0.01	< 0.05	< 0.05
MC3R:NMUR2	−9.00 ± 0.02	−9.33 ± 0.07	−9.28 ± 0.02	< 0.05	< 0.05
MC3R:NPY1R	−8.37 ± 0.01	−8.71 ± 0.02	−8.76 ± 0.03	< 0.01	< 0.001
MC3R:OXTR	−9.09 ± 0.07	−9.39 ± 0.03	−9.76 ± 0.02	< 0.05	< 0.01
MC3R:PRLH	−8.89 ± 0.01	−9.14 ± 0.07	−9.31 ± 0.03	< 0.05	< 0.05
MC3R:PTGER3	−9.22 ± 0.03	−9.59 ± 0.04	−9.16 ± 0.09	< 0.05	NS
MC3R:SSTR1	−8.89 ± 0.01	−9.49 ± 0.15	−9.43 ± 0.07	< 0.05	< 0.05

One-way ANOVA was applied in the statistical analysis.

Table 4 – Statistical analysis of competitive binding curve of MC4R.

	LogIC50			P value	
	1:0	1:3	1:6	1:0 vs 1:3	1:0 vs 1:6
MC4R:CXCR4	−9.79 ± 0.01	−10.40 ± 0.10	−10.65 ± 0.15	< 0.05	< 0.05
MC4R:HTR2C	−9.65 ± 0.02	−9.59 ± 0.06	−9.48 ± 0.12	NS	< 0.05
MC4R:NMUR2	−9.79 ± 0.02	−10.48 ± 0.07	−10.20 ± 0.03	< 0.0001	< 0.001
MC4R:NPFFR1	−9.71 ± 0.04	−10.07 ± 0.05	−10.48 ± 0.01	< 0.0001	< 0.0001
MC4R:NPY5R	−9.60 ± 0.28	−10.79 ± 0.23	−10.55 ± 0.17	< 0.01	< 0.001
MC4R:PROKR1	−9.69 ± 0.12	−10.21 ± 0.01	−10.51 ± 0.37	NS	< 0.01
MC4R:PTGER1	−9.93 ± 0.07	−10.29 ± 0.06	−10.39 ± 0.19	NS	< 0.01
MC4R:PTGER3	−10.37 ± 0.03	−10.94 ± 0.09	−12.29 ± 1.06	NS	< 0.05
MC4R:SSTR1	−9.85 ± 0.36	−12.46 ± 1.67	−13.41 ± 0.67	< 0.05	< 0.05
MC4R:SSTR2	−9.79 ± 0.02	−10.33 ± 0.10	−10.03 ± 0.20	< 0.05	NS
MC4R:SSTR3	−10.30 ± 0.12	−10.86 ± 0.11	−10.89 ± 0.08	NS	< 0.05

One-way ANOVA was applied in the statistical analysis.

constitutive activity. Similar results from another study indicate that MC3R could change the basal activity of GHSR [38]. Unlike with MC3R, we find that only GPR146 and HTR2C increase the accumulation of cAMP in MC4R, and HTR2C changes the constitutive activity of the $\text{G}\alpha_s$ pathway. We speculated that these phenomena might be caused by the distinct neuronal nucleuses of MC3R and MC4R in the regulation of energy metabolism within the hypothalamus [55,70]. Constitutive activity of MC4R maintained by the N-terminal domain showed unique properties [71]; here, HTR2C increased the basal activity of MC4R, possibly by involvement of the N-terminal domain of MC4R in the heterodimers. Next, we assessed the pharmacological impact of heterodimerization of GPCRs on signal transduction by competitive binding and surface

ELISA assay, as heterodimerization may change the ligand affinity of GPCR and the expression level on the membrane surface. Previous studies on GPCR dimers reported that interaction with muscarinic/adrenergic receptors alpha 2/m3 and m3/alpha 2 restored the high-affinity agonist binding [72]. Similarly, GABA_B receptors increased their agonist affinity when both receptor subtypes were co-expressed [73,74]. As a cyclic peptide antagonist of MC4R, SHU9119 was chosen as the competitive ligand for α -MSH. The administration of SHU9119 could block the inhibitory effect of α -MSH on food intake [75]. Our results indicated that multiple GPCRs changed the antagonism of MC3R and MC4R, which might be caused by changes in ligand affinity. In terms of membrane surface expression, we found

that it was common for GPCRs to affect the membrane surface expression levels of MC3R and MC4R, suggesting that the formation of heterodimers occur before cell surface delivery. Other research also demonstrated that GPCR dimerization is required for receptor maturation and cell surface delivery in endoplasmic reticulum and the Golgi apparatus [76,77].

It is well known that co-expression of GPCR partners in the same cell within native tissue is an important prerequisite for the formation of the GPCR heterodimer *in vivo*. To check whether Mc3r, Mc4r and the 43 selected GPCRs co-express in the same cell, we evaluated the expression levels of these GPCRs with Mc3r ([Supplementary Figure 7](#)) and Mc4r ([Supplementary Figure 8](#)) in the same cell using the integrative mouse hypothalamic single cell transcriptome data. The results suggested that 40 out of 43 selected GPCRs were found to co-express with Mc3r and Mc4r. However, 3 selected GPCRs (Ffar1, Gpr63 and Prokr1) were not detected in the Mc3r-positive cell, and 4 selected GPCRs (Ffar1, Gpr63, Prokr1 and Glp1r) were not co-expressed with Mc4r. No gene expression detected for a few GPCRs in Mc3r/Mc4r positive cells has two possible explanations: (1) they are actually not co-expressed with Mc3r/Mc4r in the mouse hypothalamus, suggesting that the heterodimerizations of these GPCRs with Mc3r/Mc4r are unlikely *in vivo*; and (2) the failure to detect co-expression of these GPCRs with Mc3r/Mc4r may be caused by the limitations of sequencing depth and gene detection in single cell RNA-seq technology. Altogether, as all of these GPCR partners of Mc3r and Mc4r were based on bioinformatic analysis and *in vitro* experiment validation in non-neuronal cell lines, the application of these findings *in vivo*, especially in the hypothalamus, still needs further examination in our future studies.

In conclusion, we reported the key interacting GPCR candidates of melanocortin signaling in the central nervous system by performing integrative analysis of mouse hypothalamic scRNA-Seq datasets, functional enrichment analysis and *in vitro* experimental screenings. Our findings could establish a composite fine physiologically regulatory network of GPCR-associated endocrine circuits in the central nervous system.

ACKNOWLEDGMENTS

The work was supported by grants from the National Key Research and Development Program of China (Grant No. 2017YFA0103902 & 2019YFA0111400); The National Natural Science Foundation of China (Grant No. 31771283); the Innovative Research Team of High-level Local Universities in Shanghai (Grant No. SSMU-ZDCX20180700) and the Key Laboratory Program of the Education Commission of Shanghai Municipality (Grant No. ZDSYS14005).

CONFLICT OF INTEREST

None declared.

APPENDIX A. SUPPLEMENTARY DATA

Supplementary data to this article can be found online at <https://doi.org/10.1016/j.molmet.2021.101317>.

REFERENCES

- [1] Whalen, E.J., Rajagopal, S., Lefkowitz, R.J., 2011. Therapeutic potential of β -arrestin- and G protein-biased agonists. *Trends in Molecular Medicine* 17(3): 126–139.
- [2] Tao, Y.X., 2020. Molecular chaperones and G protein-coupled receptor maturation and pharmacology. *Molecular and Cellular Endocrinology* 511:110862.
- [3] Milligan, G., 2004. G protein-coupled receptor dimerization: function and ligand pharmacology. *Molecular Pharmacology* 66(1):1–7.
- [4] Angers, S., Salahpour, A., Joly, E., Hilairret, S., Chelsky, D., Dennis, M., et al., 2000. Detection of beta 2-adrenergic receptor dimerization in living cells using bioluminescence resonance energy transfer (BRET). *Proceedings of the National Academy of Sciences of the U.S.A.* 97(7):3684–3689.
- [5] Milligan, G., Canals, M., Pediani, J.D., Ellis, J., Lopez-Gimenez, J.F., 2006. The role of GPCR dimerisation/oligomerisation in receptor signalling. *Ernst Schering Found Symp Proc*(2):145–161.
- [6] Smith, N.J., Milligan, G., 2010. Allostery at G protein-coupled receptor homo- and heteromers: uncharted pharmacological landscapes. *Pharmacological Reviews* 62(4):701–725.
- [7] Satake, H., Matsubara, S., Aoyama, M., Kawada, T., Sakai, T., 2013. GPCR heterodimerization in the reproductive system: functional regulation and implication for biodiversity. *Frontiers in Endocrinology* 4:100.
- [8] Bouvier, M., 2001. Oligomerization of G-protein-coupled transmitter receptors. *Nature Reviews Neuroscience* 2(4):274–286.
- [9] George, S.R., O'Dowd, B.F., Lee, S.P., 2002. G-protein-coupled receptor oligomerization and its potential for drug discovery. *Nature Reviews Drug Discovery* 1(10):808–820.
- [10] Li, L., Liang, J., Zhang, C., Liu, T., Zhang, C., 2021. Peripheral actions and direct central-local communications of melanocortin 4 receptor signaling. *Journal of Sport Health Science*.
- [11] Cone, R.D., 2006. Studies on the physiological functions of the melanocortin system. *Endocrine Reviews* 27(7):736–749.
- [12] Tao, Y.X., Yuan, Z.H., Xie, J., 2013. G protein-coupled receptors as regulators of energy homeostasis. *Progress in Molecular Biology Translational Science* 114:1–43.
- [13] Panaro, B.L., Tough, I.R., Engelstoft, M.S., Matthews, R.T., Digby, G.J., Møller, C.L., et al., 2014. The melanocortin-4 receptor is expressed in enteroendocrine L cells and regulates the release of peptide YY and glucagon-like peptide 1 *in vivo*. *Cell Metabolism* 20(6):1018–1029.
- [14] Cone, R.D., 2005. Anatomy and regulation of the central melanocortin system. *Nature Neuroscience* 8(5):571–578.
- [15] Renquist, B.J., Lippert, R.N., Sebag, J.A., Ellacott, K.L., Cone, R.D., 2011. Physiological roles of the melanocortin MC₃ receptor. *European Journal of Pharmacology* 660(1):13–20.
- [16] Hentges, S.T., Otero-Corcho, V., Pennock, R.L., King, C.M., Low, M.J., 2009. Proopiomelanocortin expression in both GABA and glutamate neurons. *Journal of Neuroscience* 29(43):13684–13690.
- [17] Andermann, M.L., Lowell, B.B., 2017. Toward a wiring diagram understanding of appetite control. *Neuron* 95(4):757–778.
- [18] Rossi, M.A., Stuber, G.D., 2018. Overlapping brain circuits for homeostatic and hedonic feeding. *Cell Metabolism* 27(1):42–56.
- [19] Al-Qassab, H., Smith, M.A., Irvine, E.E., Guillermet-Guibert, J., Claret, M., Choudhury, A.I., et al., 2009. Dominant role of the p110beta isoform of PI3K over p110alpha in energy homeostasis regulation by POMC and AgRP neurons. *Cell Metabolism* 10(5):343–354.
- [20] Xu, Y., Elmquist, J.K., Fukuda, M., 2011. Central nervous control of energy and glucose balance: focus on the central melanocortin system. *Annals of the New York Academy of Sciences* 1243:1–14.
- [21] Yang, L.K., Tao, Y.X., 2017. Biased signaling at neural melanocortin receptors in regulation of energy homeostasis. *Biochimica et Biophysica Acta - Molecular Basis of Disease* 1863(10 Pt A):2486–2495.
- [22] Mountjoy, K.G., Mortrud, M.T., Low, M.J., Simerly, R.B., Cone, R.D., 1994. Localization of the melanocortin-4 receptor (MC4-R) in neuroendocrine and autonomic control circuits in the brain. *Molecular Endocrinology* 8(10):1298–1308.

- [23] Jégou, S., Boutelet, I., Vaudry, H., 2000. Melanocortin-3 receptor mRNA expression in pro-opiomelanocortin neurones of the rat arcuate nucleus. *Journal of Neuroendocrinology* 12(6):501–505.
- [24] Yang, Z., Tao, Y.X., 2016. Biased signaling initiated by agouti-related peptide through human melanocortin-3 and -4 receptors. *Biochimica et Biophysica Acta* 1862(9):1485–1494.
- [25] Zhang, C., Forlano, P.M., Cone, R.D., 2012. AgRP and POMC neurons are hypophysiotropic and coordinately regulate multiple endocrine axes in a larval teleost. *Cell Metabolism* 15(2):256–264.
- [26] Biebermann, H., Kühnen, P., Kleinau, G., Krude, H., 2012. The neuroendocrine circuitry controlled by POMC, MSH, and AGRP. *Handbook of Experimental Pharmacology* 209:47–75.
- [27] Wang, W., Guo, D.Y., Lin, Y.J., Tao, Y.X., 2019. Melanocortin regulation of inflammation. *Frontiers in Endocrinology* 10:683.
- [28] Renquist, B.J., Murphy, J.G., Larson, E.A., Olsen, D., Klein, R.F., Ellacott, K.L., et al., 2012. Melanocortin-3 receptor regulates the normal fasting response. *Proceedings of the National Academy of Sciences of the U S A* 109(23):E1489–E1498.
- [29] Panaro, B.L., Cone, R.D., 2013. Melanocortin-4 receptor mutations paradoxically reduce preference for palatable foods. *Proceedings of the National Academy of Sciences of the U S A* 110(17):7050–7055.
- [30] Elsner, A., Tarnow, P., Schaefer, M., Ambrugger, P., Krude, H., Grütters, A., et al., 2006. MC4R oligomerizes independently of extracellular cysteine residues. *Peptides* 27(2):372–379.
- [31] Haqq, A.M., René, P., Kishi, T., Khong, K., Lee, C.E., Liu, H., et al., 2003. Characterization of a novel binding partner of the melanocortin-4 receptor: attractin-like protein. *Biochemical Journal* 376(Pt 3):595–605.
- [32] Sebag, J.A., Zhang, C., Hinkle, P.M., Bradshaw, A.M., Cone, R.D., 2013. Developmental control of the melanocortin-4 receptor by MRAP2 proteins in zebrafish. *Science* 341(6143):278–281.
- [33] Tai, X., Xue, S., Zhang, C., Liu, Y., Chen, J., Han, Y., et al., 2021. Pharmacological evaluation of MRAP proteins on *Xenopus* neural melanocortin signaling. *Journal of Cellular Physiology*.
- [34] Li, L., Xu, Y., Zheng, J., Kuang, Z., Zhang, C., Li, N., et al., 2021. Pharmacological modulation of dual melanocortin-4 receptor signaling by melanocortin receptor accessory proteins in the *Xenopus laevis*. *Journal of Cellular Physiology*.
- [35] Wen, Z.Y., Liu, T., Qin, C.J., Zou, Y.C., Wang, J., Li, R., et al., 2021. MRAP2 interaction with melanocortin-4 receptor in SnakeHead (*Channa argus*). *Biomolecules* 11(3).
- [36] Wang, M., Chen, Y., Zhu, M., Xu, B., Guo, W., Lyu, Y., et al., 2019. Pharmacological modulation of melanocortin-4 receptor by melanocortin receptor accessory protein 2 in Nile tilapia. *General and Comparative Endocrinology* 282:113219.
- [37] Zhu, M., Xu, B., Wang, M., Liu, S., Zhang, Y., Zhang, C., 2019. Pharmacological modulation of MRAP2 protein on melanocortin receptors in the sea lamprey. *Endocr Connect* 8(4):378–388.
- [38] Rediger, A., Piechowski, C.L., Yi, C.X., Tarnow, P., Strotmann, R., Grütters, A., et al., 2011. Mutually opposite signal modulation by hypothalamic heterodimerization of ghrelin and melanocortin-3 receptors. *Journal of Biological Chemistry* 286(45):39623–39631.
- [39] Robinson, S.W., Dinulescu, D.M., Cone, R.D., 2000. Genetic models of obesity and energy balance in the mouse. *Annual Review of Genetics* 34:687–745.
- [40] Tecott, L.H., Sun, L.M., Akana, S.F., Strack, A.M., Lowenstein, D.H., Dallman, M.F., et al., 1995. Eating disorder and epilepsy in mice lacking 5-HT2c serotonin receptors. *Nature* 374(6522):542–546.
- [41] Wang, X.P., Norman, M., Yang, J., Magnusson, J., Kreienkamp, H.J., Richter, D., et al., 2006. Alterations in glucose homeostasis in SSTR1 gene-ablated mice. *Molecular and Cellular Endocrinology* 247(1–2):82–90.
- [42] Chamorro, S., Della-Zuana, O., Fauchère, J.L., Féletalou, M., Galizzi, J.P., Levens, N., 2002. Appetite suppression based on selective inhibition of NPY receptors. *International Journal of Obesity and Related Metabolic Disorders* 26(3):281–298.
- [43] Seong, J., Kang, J.Y., Sun, J.S., Kim, K.W., 2019. Hypothalamic inflammation and obesity: a mechanistic review. *Archives of Pharmacal Research* 42(5):383–392.
- [44] Anderson, E.J., Çakir, I., Carrington, S.J., Cone, R.D., Ghamari-Langroudi, M., Gillyard, T., et al., 2016. 60 years OF POMC: regulation of feeding and energy homeostasis by α -MSH. *Journal of Molecular Endocrinology* 56(4):T157–T174.
- [45] Chen, R., Wu, X., Jiang, L., Zhang, Y., 2017. Single-cell RNA-seq reveals hypothalamic cell diversity. *Cell Reports* 18(13):3227–3241.
- [46] Rossi, M.A., Basiri, M.L., McHenry, J.A., Kosyk, O., Otis, J.M., van den Munkhof, H.E., et al., 2019. Obesity remodels activity and transcriptional state of a lateral hypothalamic brake on feeding. *Science* 364(6447):1271–1274.
- [47] Romanov, R.A., Zeisel, A., Bakker, J., Girach, F., Hellysaz, A., Tomer, R., et al., 2017. Molecular interrogation of hypothalamic organization reveals distinct dopamine neuronal subtypes. *Nature Neuroscience* 20(2):176–188.
- [48] Mickelsen, L.E., Bolisetty, M., Chimileski, B.R., Fujita, A., Beltrami, E.J., Costanzo, J.T., et al., 2019. Single-cell transcriptomic analysis of the lateral hypothalamic area reveals molecularly distinct populations of inhibitory and excitatory neurons. *Nature Neuroscience* 22(4):642–656.
- [49] He, Q., Mok, T.N., Yun, L., He, C., Li, J., Pan, J., 2020. Single-cell RNA sequencing analysis of human kidney reveals the presence of ACE2 receptor: a potential pathway of COVID-19 infection. *Mol Genet Genomic Med* 8(10):e1442.
- [50] Zhou, R.S., Zhang, E.X., Sun, Q.F., Ye, Z.J., Liu, J.W., Zhou, D.H., et al., 2019. Integrated analysis of lncRNA-miRNA-mRNA ceRNA network in squamous cell carcinoma of tongue. *BMC Cancer* 19(1):779.
- [51] Pesenti, C., Navone, S.E., Guaraccia, L., Terrasi, A., Costanza, J., Silipigni, R., et al., 2019. The genetic landscape of human glioblastoma and matched primary cancer stem cells reveals intratumour similarity and intertumour heterogeneity. *Stem Cells International*, 2617030, 2019.
- [52] Butler, A.A., Kesterson, R.A., Khong, K., Cullen, M.J., Pelleymounter, M.A., Dekoning, J., et al., 2000. A unique metabolic syndrome causes obesity in the melanocortin-3 receptor-deficient mouse. *Endocrinology* 141(9):3518–3521.
- [53] Chen, A.S., Marsh, D.J., Trumbauer, M.E., Frazier, E.G., Guan, X.M., Yu, H., et al., 2000. Inactivation of the mouse melanocortin-3 receptor results in increased fat mass and reduced lean body mass. *Nature Genetics* 26(1):97–102.
- [54] Tao, Y.X., 2010. Mutations in the melanocortin-3 receptor (MC3R) gene: impact on human obesity or adiposity. *Current Opinion in Investigational Drugs* 11(10):1092–1096.
- [55] Huszar, D., Lynch, C.A., Fairchild-Huntress, V., Dunmore, J.H., Fang, Q., Berkemeier, L.R., et al., 1997. Targeted disruption of the melanocortin-4 receptor results in obesity in mice. *Cell* 88(1):131–141.
- [56] Balthasar, N., Dalgaard, L.T., Lee, C.E., Yu, J., Funahashi, H., Williams, T., et al., 2005. Divergence of melanocortin pathways in the control of food intake and energy expenditure. *Cell* 123(3):493–505.
- [57] Sohn, J.W., Elmquist, J.K., Williams, K.W., 2013. Neuronal circuits that regulate feeding behavior and metabolism. *Trends in Neurosciences* 36(9):504–512.
- [58] Cowley, M.A., Smart, J.L., Rubinstein, M., Cerdán, M.G., Diano, S., Horvath, T.L., et al., 2001. Leptin activates anorexigenic POMC neurons through a neural network in the arcuate nucleus. *Nature* 411(6836):480–484.
- [59] Atasoy, D., Betley, J.N., Su, H.H., Sternson, S.M., 2012. Deconstruction of a neural circuit for hunger. *Nature* 488(7410):172–177.
- [60] Vennemann, A., Gerstner, A., Kern, N., Ferreiros Bouzas, N., Narumiya, S., Maruyama, T., et al., 2012. PTGS-2-PTGER2/4 signaling pathway partially protects from diabetogenic toxicity of streptozotocin in mice. *Diabetes* 61(7):1879–1887.
- [61] Choudhary, S., Blackwell, K., Voznesensky, O., Deb Roy, A., Pilbeam, C., 2013. Prostaglandin E2 acts via bone marrow macrophages to block PTH-stimulated osteoblast differentiation in vitro. *Bone* 56(1):31–41.

- [62] Kasahara, Y., Sato, K., Takayanagi, Y., Mizukami, H., Ozawa, K., Hideya, S., et al., 2013. Oxytocin receptor in the hypothalamus is sufficient to rescue normal thermoregulatory function in male oxytocin receptor knockout mice. *Endocrinology* 154(11):4305–4315.
- [63] Johansson, A., 2016. Evolution of physicochemical properties of melanin concentrating hormone receptor 1 (MCHr1) antagonists. *Bioorganic & Medicinal Chemistry Letters* 26(19):4559–4564.
- [64] Xu, Y., Jones, J.E., Kohno, D., Williams, K.W., Lee, C.E., Choi, M.J., et al., 2008. 5-HT2CRs expressed by pro-opiomelanocortin neurons regulate energy homeostasis. *Neuron* 60(4):582–589.
- [65] Lau, J., Farzi, A., Enriquez, R.F., Shi, Y.C., Herzog, H., 2017. GPR88 is a critical regulator of feeding and body composition in mice. *Scientific Reports* 7(1):9912.
- [66] Han, F., Liu, X., Chen, C., Liu, Y., Du, M., Zhou, Y., et al., 2020. Hypercholesterolemia risk-associated GPR146 is an orphan G-protein coupled receptor that regulates blood cholesterol levels in humans and mice. *Cell Research* 30(4):363–365.
- [67] Soni, A., Amisten, S., Rorsman, P., Salehi, A., 2013. GPRC5B a putative glutamate-receptor candidate is negative modulator of insulin secretion. *Biochemical and Biophysical Research Communications* 441(3):643–648.
- [68] Brock, C., Oueslati, N., Soler, S., Boudier, L., Rondard, P., Pin, J.P., 2007. Activation of a dimeric metabotropic glutamate receptor by intersubunit rearrangement. *Journal of Biological Chemistry* 282(45):33000–33008.
- [69] Damian, M., Martin, A., Mesnier, D., Pin, J.P., Banères, J.L., 2006. Asymmetric conformational changes in a GPCR dimer controlled by G-proteins. *The EMBO Journal* 25(24):5693–5702.
- [70] Roselli-Rehfuss, L., Mountjoy, K.G., Robbins, L.S., Mortrud, M.T., Low, M.J., Tatro, J.B., et al., 1993. Identification of a receptor for gamma melanotropin and other proopiomelanocortin peptides in the hypothalamus and limbic system. *Proceedings of the National Academy of Sciences of the U S A* 90(19):8856–8860.
- [71] Ersoy, B.A., Pardo, L., Zhang, S., Thompson, D.A., Millhauser, G., Govaerts, C., et al., 2012. Mechanism of N-terminal modulation of activity at the melanocortin-4 receptor GPCR. *Nature Chemical Biology* 8(8):725–730.
- [72] Maggio, R., Vogel, Z., Wess, J., 1993. Coexpression studies with mutant muscarinic/adrenergic receptors provide evidence for intermolecular "cross-talk" between G-protein-linked receptors. *Proceedings of the National Academy of Sciences of the U S A* 90(7):3103–3107.
- [73] White, J.H., Wise, A., Main, M.J., Green, A., Fraser, N.J., Disney, G.H., et al., 1998. Heterodimerization is required for the formation of a functional GABA(B) receptor. *Nature* 396(6712):679–682.
- [74] Kuner, R., Köhr, G., Grünwald, S., Eisenhardt, G., Bach, A., Kornau, H.C., 1999. Role of heteromer formation in GABAB receptor function. *Science* 283(5398):74–77.
- [75] Fan, W., Boston, B.A., Kesterson, R.A., Hruby, V.J., Cone, R.D., 1997. Role of melanocortinergic neurons in feeding and the agouti obesity syndrome. *Nature* 385(6612):165–168.
- [76] Law, P.Y., Erickson-Herbrandon, L.J., Zha, Q.Q., Solberg, J., Chu, J., Sarre, A., et al., 2005. Heterodimerization of mu- and delta-opioid receptors occurs at the cell surface only and requires receptor-G protein interactions. *Journal of Biological Chemistry* 280(12):11152–11164.
- [77] Bulenger, S., Marullo, S., Bouvier, M., 2005. Emerging role of homo- and heterodimerization in G-protein-coupled receptor biosynthesis and maturation. *Trends in Pharmacological Sciences* 26(3):131–137.